

Accepted Manuscript

A novel in vitro method to model the fate of subcutaneously administered biopharmaceuticals and associated formulation components

Hanne M. Kinnunen, Vikas Sharma, Luis Rodrigo Contreras-Rojas, Yafei Yu, Chlöe Alleman, Alavattam Sreedhara, Stefan Fischer, Leslie Khawli, Stefan T. Yohe, Daniela Bumbaca, Thomas W. Patapoff, Ann L. Daugherty, Randall J. Mersny

PII: S0168-3659(15)30029-8
DOI: doi: [10.1016/j.jconrel.2015.07.016](https://doi.org/10.1016/j.jconrel.2015.07.016)
Reference: COREL 7763

To appear in: *Journal of Controlled Release*

Received date: 29 May 2015
Revised date: 13 July 2015
Accepted date: 15 July 2015

Please cite this article as: Hanne M. Kinnunen, Vikas Sharma, Luis Rodrigo Contreras-Rojas, Yafei Yu, Chlöe Alleman, Alavattam Sreedhara, Stefan Fischer, Leslie Khawli, Stefan T. Yohe, Daniela Bumbaca, Thomas W. Patapoff, Ann L. Daugherty, Randall J. Mersny, A novel in vitro method to model the fate of subcutaneously administered biopharmaceuticals and associated formulation components, *Journal of Controlled Release* (2015), doi: [10.1016/j.jconrel.2015.07.016](https://doi.org/10.1016/j.jconrel.2015.07.016)

This is a PDF file of an unedited manuscript that has been accepted for publication. As a service to our customers we are providing this early version of the manuscript. The manuscript will undergo copyediting, typesetting, and review of the resulting proof before it is published in its final form. Please note that during the production process errors may be discovered which could affect the content, and all legal disclaimers that apply to the journal pertain.



A novel in vitro method to model the fate of subcutaneously administered biopharmaceuticals and associated formulation components

Hanne M. Kinnunen^a, Vikas Sharma^b, Luis Rodrigo Contreras-Rojas^a, Yafei Yu^a, Chlöe Alleman^a, Alavattam Sreedhara^b, Stefan Fischer^c, Leslie Khawli^{e, f}, Stefan T. Yohe^d, Daniela Bumbaca^e, Thomas W. Patapoff^b, Ann L. Daugherty^d, and Randall J. Mrsny^a

^aDepartment of Pharmacy and Pharmacology, University of Bath, Bath, UK

^bLate Stage Pharmaceutical Development, Genentech, Inc. South San Francisco, CA 94080, USA

^cLate Stage Pharmaceutical and Processing Development, Pharmaceutical Development & Supplies, Pharma Technical Development Biologics EU F. Hoffmann-La Roche Ltd, Basel, CH-4070, Switzerland

^dDrug Delivery, Genentech, Inc. South San Francisco, CA 94080, USA

^ePharmacokinetics, Genentech, Inc. South San Francisco, CA 94080, USA

^fCurrent address: Department of Pathology, Keck School of Medicine, University of Southern California, Los Angeles, CA 90033

Contact Info:

Prof. Randall Mrsny
University of Bath
Department of Pharmacy and Pharmacology
Claverton Down
Bath BA2 7AY UK
Tel +44 122 538 3358
Rjm37@bath.ac.uk

Current address for Dr. Hanne Kinnunen:

Durham University
Division of Pharmacy
Queen's Campus
Wolfson Building
Stockton-on-Tees TS17 6BH UK
Telephone +44 (0)191 334 0400
Email: hanne.kinnunen@durham.ac.uk

Category: Original research

Keywords: Subcutaneous injection, biopharmaceuticals, *in vitro* model, formulation design

ABSTRACT

Subcutaneous (SC) injection is becoming a more common route for the administration of biopharmaceuticals. Currently, there is no reliable *in vitro* method that can be used to anticipate the *in vivo* performance of a biopharmaceutical formulation intended for SC injection. Nor is there an animal model that can predict *in vivo* outcomes such as bioavailability in humans. We address this unmet need by the development of a novel *in vitro* system, termed Scissor (Subcutaneous Injection Site Simulator). The system models environmental changes that a biopharmaceutical could experience as it transitions from conditions of a drug product formulation to the homeostatic state of the hypodermis following SC injection. Scissor uses a dialysis-based injection chamber, which can incorporate various concentrations and combinations of acellular extracellular matrix (ECM) components that may affect the release of a biopharmaceutical from the SC injection site. This chamber is immersed in a container of a bicarbonate-based physiological buffer that mimics the SC injection site and the infinite sink of the body, respectively. Such an arrangement allows for real-time monitoring of the biopharmaceutical within the injection chamber that can be used to characterize physicochemical changes of the drug and its interactions with ECM components. Movement of a biopharmaceutical from the injection chamber to the infinite sink compartment simulates the drug migration from the injection site and uptake by the blood and/or lymph capillaries. Here, we present an initial evaluation of the Scissor system using the ECM element hyaluronic acid and test formulations of insulin and four different monoclonal antibodies. Our findings suggest that Scissor can provide a tractable method to examine the potential fate of a biopharmaceutical formulation after its SC injection in humans and that this approach may provide a reliable and representative alternative to animal testing for the initial screening of SC formulations.

INTRODUCTION

More than forty years after the innovative application of recombinant DNA technology to produce novel protein therapeutics, the biotechnology industry has fulfilled its promise of safely and effectively treating unmet medical needs and providing life saving therapies. Indeed, many diseases can now be treated as a chronic condition rather than an acute malady with a poor prognosis¹. As there is strong patient preference for subcutaneous (SC) injections over the more time-intensive intravenous (IV) infusion therapies², many biopharmaceuticals under development as well as those previously approved as IV therapies are being formulated for SC injection. While IV administration is considered to consistently provide the optimal means of delivering the entirety of a dose to a patient, molecules dosed by the SC route typically have a lower bioavailability. Currently, it is impossible to predict the extent of this diminished bioavailability and to determine the basis for these outcomes; the biophysical status of a SC injected protein or peptide and its possible interactions with ECM components of the hypodermis in man are not easily monitored. What is known is that currently approved biopharmaceutical formulations have bioavailabilities that range from 20 - 100%³, depending on the drug, with published data on the bioavailability of monoclonal antibodies in man suggests absorption between 50-100%⁴. Efforts to find animal models that universally and reliably predict human SC bioavailabilities have been unsuccessful⁵. For example, the SC bioavailability of human epoetin- β is 80% in dogs, 76% in rats, and 70% in mice⁶ but only 20-36% in man^{7,8}; interferon- α has a 42% BA in dogs⁹ but >80% in man¹⁰ following SC injection.

In order to enter the systemic circulation and reach intended therapeutic targets throughout the body, SC injected biopharmaceuticals must be absorbed, presumably by uptake into blood or lymph capillaries^{11,12}. Besides specific receptors possibly being present on cells at or near the injection site, uptake into the circulation appears to be dictated by the physicochemical properties of the molecule such as hydrodynamic radius, net charge, and hydrophobic characteristics¹³. A commercially acceptable

biopharmaceutical product is typically stable for two years at 5 °C and has a high drug concentration to allow for a less than 1 cc injection volume; formulations are commonly at pH 5-6.5 and contains stabilizing excipients such as surfactants (e.g. polysorbates), poly-alcohols (e.g. mannitol), tonicifiers (e.g., salts and sugars), and sometime a preservative. Over a time frame of minutes to hours after SC injection, the biopharmaceutical will experience potentially stressful events; sometimes including a transition through its isoelectric point as the local environment shifts from conditions of the drug product formulation to that of the hypodermis as the SC injection site regains its homeostatic state. Diffusion of a biopharmaceutical from the SC injection site may also be affected by biophysical changes induced by this transition and interaction(s) with extracellular matrix (ECM) components. Efforts made to disorganize the ECM environment and improve the outcome of SC injections support the criticality of interactions with non-cellular ECM elements affecting the overall fate of a SC injected biopharmaceutical^{14,15}. Thus, we have hypothesized that a primary factor driving SC bioavailability achieved for a given formulation involves the stability of the biopharmaceutical at physiological conditions and its interactions with ECM components.

We have established a novel *in vitro* system to model these early events and to simulate dynamic processes imposed on a biopharmaceutical as it transitions from a drug product formulation to the physiological conditions of the hypodermis. Our approach utilizes current information on the physiological properties of the hypodermis for factors such as ECM components, pH, ionic composition, interstitial pressure, and temperature¹⁶. While the hypodermis also contains adipocytes and a sparse distribution of fibroblasts and macrophages, the high concentration at which most biopharmaceuticals are administered would overwhelm the capacity of these cells to exert a significant effect, magnifying the potential impact of these acellular components. In this report we present a series of studies using this *in vitro* subcutaneous injection site simulator system, termed “Scissor”, to model some of the events that might affect the fate of a

biopharmaceutical formulation components following a SC injection. Real-time measurements were made to monitor the status of the injection chamber compartment; the extent of a biopharmaceutical released into the infinite sink was determined in samples removed at specific times. The tractable nature of Scissor allows for the identification of specific factors that could affect the diffusion or stability of a biopharmaceutical after its introduction into the injection chamber and further, to assess the impact of formulation changes with the aim of developing a more rational formulation selection strategy for a biopharmaceutical that includes events that might occur after SC injection.

MATERIALS AND METHODS

Materials

Buffers were made using NaCl, KCl, CaCl₂, MgCl₂, NaHCO₃, K₂HPO₄, Na₂HPO₄ and Na₂SO₄ purchased from Sigma (Gillingham, UK). Acetonitrile, pyridine, ethanol, *m*-cresol, acetic acid, and hydrochloric acid were of HPLC quality and purchased from Sigma (Waltham, MA, USA.). Hyaluronic acid (HA) sodium salt isolated from *Streptococcus equii* with an average molecular weight of 1.5 to 1.8 MDa was obtained from Sigma (Gillingham, UK). Hyaluronidase (HAase) isolated from bovine testes, fluorescently labelled dextrans, methylene blue, 4-aminofluorescein and 3-(3-Dimethylaminopropyl)-1-ethylcarbodiimide and citric acid were all purchased from Sigma (Gillingham, UK). Bradford reagent, Pierce Slide-a-lyzer dialysis cassettes, Biodesign 14,000 molecular weight cut-off dialysis tubing, and phosphate buffered saline (PBS) tablets were purchased from Fisher (Loughborough, UK). The Dermaroller™ device was purchased from AesthetiCare (Wetherby, UK). Water was reverse osmosis purified (Millipore, France). The monoclonal antibodies anonymized as mAb 2, mAb F, mAb T and mAb A were supplied by Genentech, Inc. (South San Francisco, USA). Insuman Comb 50 (Sanofi Aventis) was purchased from AAH Pharmaceuticals (Coventry, UK). Recombinant human insulin (100

IU/mL) obtained from Sigma (Gillingham, UK) was formulated at pH 4 or at pH 7.4 in 0.1 M citric acid or 0.2 M Na₂HPO₄ buffers, respectively. In addition, each insulin formulation contained 16 mg/mL glycerol, 2.5 mg/mL m-cresol and 0.015 mg/mL Zn²⁺; all from Sigma (Gillingham, UK).

Methods

Fluorescent labelling of HA

Hyaluronic acid was fluorescently labelled following the protocol of Ogamo *et al*¹⁷. Briefly, 200 mg of sodium salt of hyaluronic acid was dissolved in 20 mL of 3:1 (v/v) mixture of 1M HCl and pyridine. 114 mg of 5-aminofluorescein (5-AF) was dissolved in 4 mL of the same solvent and the solution was then added to the HA solution. The pH of the mixture was adjusted to pH 7.4 with 12 M HCl. 0.34 g of 3-(3-Dimethylaminopropyl)-1-ethyl-carbodiimide HCl was then added to the reaction mixture while the pH was maintained at 7.4 by addition of 6M HCl. The reaction mixture was stirred in room temperature for one hour. To purify the fluorescent-HA, the reaction mixture was dialysed against 1 L of cold water for 24 h followed by a wash with 100 mL of cold ethanol, which was then dissolved in 100 mL of deionised water and freeze-dried. The resulting solid was reconstituted in water at 5 mg/mL for use.

Description of the *in vitro* system

Transparent 14 kDa MWCO dialysis tubing (Bioscience, Carmel, NY USA) was modified by puncturing a series of holes of approximately 150 µm by 50 µm in a grid pattern of 3mm x 3 mm using a stainless steel fine bore Dermaroller™ microneedle roller device. A Slide-a-lyzer® dialysis cassette was disassembled and the original membranes removed. Holes were drilled into the plastic frame of the dialysis cassette to allow replacement of the membranes with the modified Bioscience dialysis membrane and securing it in place using plastic screws and nuts. Holes drilled into the cassette were also used to facilitate the

introduction of a pH probe and a needle for introduction of test formulations. The cassette was then filled with a physiological buffer containing HA at a final concentration of 1, 5, or 10 mg/mL. The physiologic buffers was composed of 6.4 g NaCl, 0.09 g $\text{MgCl}_2 \cdot 6\text{H}_2\text{O}$, 0.4 g KCl, 0.2 g CaCl_2 and 2.1 g NaHCO_3 in 1 L H_2O CO_2 , having a calculated osmolarity of ~ 280 mOsm/L, as described by Kay *et al*¹⁸.

A glass beaker containing 300 mL of the physiological buffer solution that was heated to and maintained at 34°C, and stabilized at pH 7.4 with gaseous CO_2 , was placed in a Milton Roy Spectronic 601 spectrophotometer (Pont-Saint-Pierre, France). The modified dialysis cassette was positioned inside the beaker so that light path of the Milton Roy Spectronic 601 spectrophotometer could be used to monitor light transmittance at the simulated injection site within the cassette. A micro pH probe (Orion Micro, Thermo Scientific, Waltham, MA) connected to a Hanna Instruments HI3220 pH meter (Woonsocket, RI, USA) was placed into the cassette to be adjacent to the site of an introduced biopharmaceutical formulation but not in the spectrophotometer light path. The pH meter and spectrophotometer were connected to a computer and the measurement readings from both instruments were monitored in real-time during an experiment and recorded using a LabVIEW program (National Instruments Corporations, Austin, TX). To determine time-concentration profiles of a chemical species reaching the infinite sink buffer bath from the cassette, a baseline sample was taken from the buffer bath prior to the introduction of a 0.5 mL formulation into the injection site using a syringe and a suitable gauge hypodermic needle. Subsequent aliquots were taken from the buffer bath at selected time points.

Analytical methods

Sample separation by size exclusion high performance liquid chromatography (SE-HPLC) using the mobile phase of 0.2 M potassium phosphate buffer at pH 6.2 with 0.25 M KCl pumped at a flow rate of 1 mL/min and detection at 214 nm was used to analyze mAb

samples; samples (50 μL) were injected into a 300mm x 7.8 mm I.D., 3 μm particle size, Yarra-3000 column (Phenomenex Ltd, Macclesfield, UK) maintained at 25°C.

Insulin was detected at 214 nm using the HPLC method specified by the Pharmacopoeia¹⁹. Briefly, a Thermo Scientific Acclaim 120 C₁₈ reversed-phase column with a particle size of 5 μm , inner diameter 4.6 mm and a length of 250mm column (Fisher, Loughborough, UK) was used for the analysis at room temperature. Mobile phase A consisted of 28.4 g/L anhydrous sodium sulfate in deionized water (pH 2.3) and mobile Phase B consisted of 55 parts of mobile phase A and 45 parts of acetonitrile. The final mobile phase was prepared by mixing 42 volumes of mobile phase A and 58 volumes of mobile phase B. Samples were injected as 20 μL volumes.

Pressure measurements within the injection chamber were conducted with a needle tip pressure transducer from Gaeltec Devices (Dunvegan, UK). Viscosity measurements were performed on 70 μL samples using an Physica MCR 501 concentric cylinder cone and plate rheometer (Anton Paar, Graz, Austria) using the CP-25-1 measuring cell with a 25-mm diameter and 1.007° angle. Samples were protected from evaporation and maintained at 25 \pm 0.1 °C using an Anton Paar H-PTD200 Peltier system. Sample viscosity, reported as the average of stabilized viscosity measurements from three independent replicates, was determined by measuring torque every second for 60 s using a constant shear rate of 1000 s⁻¹. Anton Paar RheoPlus software was used for sample analysis and data reporting.

Human clinical trial data

Human mAb bioavailability data was obtained from studies that were conducted in accordance with the International Conference on Harmonisation E6 Guideline for Good Clinical Practice and approved by local internal review boards. Patients provided written informed consent prior to study inclusion.

Data analysis

Curves were fitted to the time-concentration profiles obtained for the different formulations with SigmaPlot software v12.5 (Systat Software Inc. London, UK) using equation 1:

$$y = \frac{B_{Max} x}{t_{1/2} + x} \quad \text{Equation 1.}$$

This model results in B_{max} and $t_{1/2}$ parameters for the maximum diffused fraction and half-life of diffusion of analytes, respectively. To enable meaningful comparison, the highest recovery for each of the mAb formulations was set to 100% and the lower recoveries normalized to values proportional to this standard. Data is presented as mean \pm standard deviation (SD).

RESULTS AND DISCUSSION

Organization of the Scissor system

Scissor was designed to recreate, in an *in vitro* setting, dynamic events that could affect the fate of a biopharmaceutical formulation delivered by subcutaneous (SC) injection *in vivo*. These dynamic events reflect the environmental changes that would occur as the SC injection site transitions from the drug product to the physiological conditions of the human hypodermis. This transition involves changes in pH, temperature, and ionic components with a loss of excipients transient pressure changes due to volume introduction - events that occur over a time frame of minutes to hours (Fig. 1A). Given these complexities, the Scissor system was developed with several components. A beaker containing 300 mL of a physiological media emulates the ion composition and pH of the hypodermis and functions as the infinite sink of the body. While the exact ionic composition of the hypodermis is difficult to know precisely, it has been reported to be

similar to serum^{20,21}, thus, the buffer used reflects this information available in the literature.

A modified dialysis cassette used as a chamber to emulate the SC injection site was positioned within the beaker containing the physiological media. The injection chamber was designed in two formats, one for injection volumes of <100 μL and the other for volumes of up to 1 mL. The injection chamber was designed so that it could be filled with different combinations and concentrations of extracellular matrix (ECM) components. The pH inside the injection chamber could be continuously monitored using a needle pH probe positioned in close approximation to the site of sample introduction achieved using a syringe and a needle combination consistent with the clinical use of these formulations (Fig. 1B).

The injection chamber/infinite sink compartment components were positioned in the single-beam spectrophotometer in such a way as to allow temperature control of the contents through the use of a heating mantle, gentle mixing using a magnetic stirring bar, and measurement of transmitted light at a selected wavelength (Fig. 1C). The system was maintained at approximately 34 °C, which is the average hypodermis temperature²² and the physiological media in the infinite sink was maintained at pH 7.4 by the addition of CO_2 (g). To monitor the amount and status of materials leaving the injection chamber the over time, 0.75 mL aliquots of solute bath chamber were taken at selected time points and assayed by HPLC protocols.

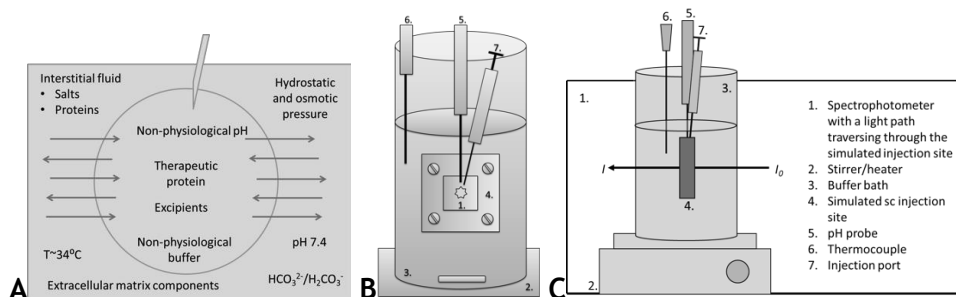


Figure 1. Dynamic events in the hypodermis following the injection of a biopharmaceutical formulation can be modeled using a modified dialysis system. A) Diagram of components and events denoting the exchange of small molecules (salts, sugars, and other excipients), buffer (transition to a bicarbonate-based environment), equilibration of temperature and pressure, and potential interaction with extracellular matrix (ECM) components. B) Cartoon depicting arrangement of positioned probes to continuously monitor pH inside and outside of the sample injection chamber and positioning of light path (crenulated circle) in a large solute bath chamber that emulates the infinite sink of the body. C) Cartoon depicting arrangement of injection chamber/infinite sink compartment in a single-beam spectrophotometer that allows for temperature control and stirring of the large bath contents. The numbering in B) and C) follows the legend shown in C).

Component Evaluation

Movement of a biopharmaceutical from the injection chamber into the infinite sink compartment would emulate migration of the drug from the injection site into the circulation as a result of local diffusion and subsequent uptake into blood capillaries and/or lymph capillaries *in vivo*. To model these two mechanisms of clearance from the SC injection site using the Scissor injection chamber, we used a 14 kDa MWCO dialysis membrane modified by a grid pattern of regularly spaced holes generated by the penetration of a Dermaroller™ microneedle roller device to represent a distribution of absorption points into lymph and blood capillaries, with a background of small molecular weight excipients diffusing through pores in the dialysis membrane (Fig. 2A). A linear correlation was observed between the log molecular weight for molecules ranging from 300 to 2,000,000 Da vs. the passive transport rate across the modified dialysis membrane (Fig. 2B). The molecular weight range selected for these studies covered the range anticipated for most biopharmaceuticals and excipients currently considered for SC injection.

We next evaluated the retention of hyaluronic acid (HA), a prominent component of the extracellular matrix (ECM), within the injection chamber. We tested this by following the release of HA labeled with 5-aminofluorescein (5-AF) using hyaluronidase (HAse) from the Scissor injection cassette. HA at 10 mg/mL was combined with a small amount of HA modified with 5-AF (<0.1%) and placed in the injection chamber. Release of 5-AF from the injection chamber, prepared using the previously described modified dialysis membrane, was monitored over time using an Omega Fluostar plate reader (Fig. 2C). After 1 h, only trace amounts of 5-AF were measured in the infinite sink compartment, suggesting that the membrane used in the Scissor system effectively restricted the efflux of HA from the injection chamber. As a positive control, 2.5 mg of HAse was injected in a 100 μ L volume of physiological buffer solution into the injection chamber after one h of monitoring HA diffusion, which resulted in a steady release of 5-AF into the infinite sink chamber (Fig. 2C).

Finally, we considered the interstitial pressure (IP) of the hypodermis as an element that might affect events associated with SC injection site outcomes. Two factors dominate hypodermis IP: fluid dynamic pressure associated with an increased volume in a defined space and colloidal osmotic pressure exerted by poly-ionic materials in proximity to a semipermeable barrier¹⁶. Measurements made of the hypodermis IP have suggested this value to be between 10-15 mm Hg^{23,24}. We used the hydrostatic pressure produced by the fluid of the infinite sink against the membrane of the injection chamber to emulate physiological pressure conditions; the dialysis cassette was placed at a depth in the beaker bath to produce a pressure in the range of 10 mm Hg as measured with a needle probe pressure transducer (Fig. 2D). Pressure measurements within the injection chamber were conducted with a needle tip pressure transducer from Gaeltec Devices. Injection of a volume relevant to a biopharmaceutical formulation produced only a minor and transient pressure shift within the dialysis

cassette (Fig. 2D).

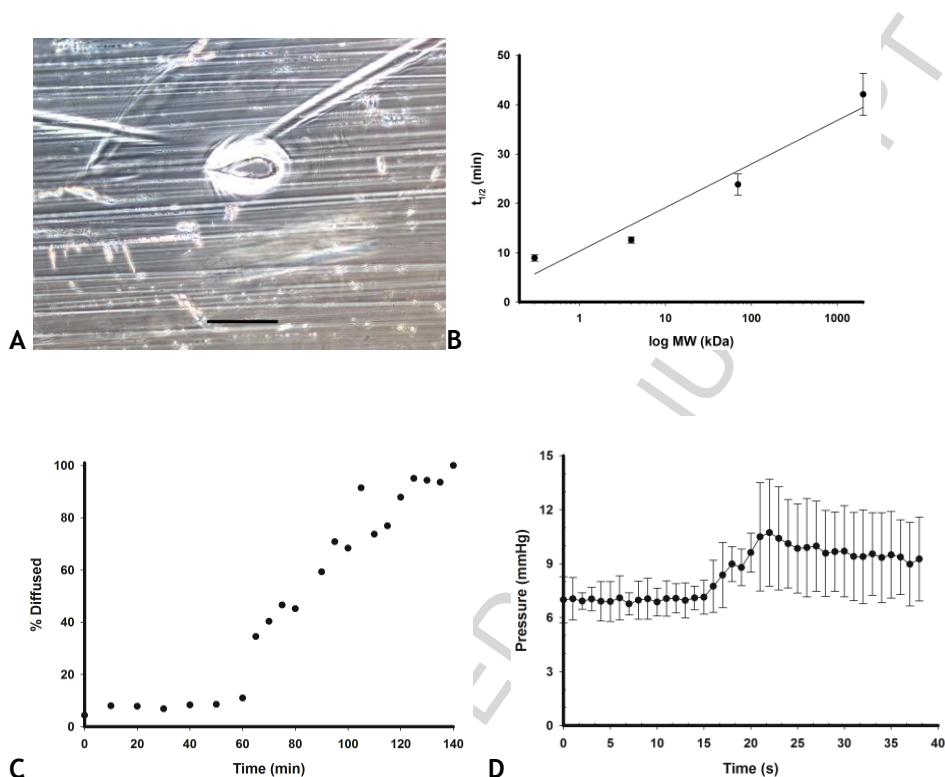


Figure 2. Characteristics of dialysis membrane and dialysis cassette matrix components. A) Optical characterization of DermarollerTM-modified dialysis membrane showing the nature of an introduced pore. Scale bar = 200 μm . B) Macromolecular flux in terms of diffusal half-life ($t_{1/2}$) across the DermarollerTM-modified dialysis membrane was linear across a wide range that is relevant for most biopharmaceuticals. C) Impact of hyaluronidase (HAase) on retention of labeled HA in the injection chamber. Release of 5-aminofluorescein that was chemically coupled to HA was monitored by detection of fluorescence in the infinite sink bath over time with HAase being added at 60 min. D) Pressure measured within the injection chamber dialysis cassette before and after an injection of 0.5 mL of water at 15 sec. The data represents average ($n=3$) \pm S.D.

Evaluation of insulin formulations using the Scissor system

Human insulin was formulated at acidic conditions and with the excipients *m*-cresol and Zn^{2+} , similar to commercial products of this biopharmaceutical²⁵, and injected into the Scissor system injection chamber that lacked ECM elements (Fig. 3A). In this case, *m*-cresol was observed to leave the injection chamber rapidly, essentially being completely absent in the injection chamber after ~ 30 min. We observed that the pH of the injection chamber dropped from neutrality to ~3.5 very rapidly and this change correlated with a striking decrease in injection chamber clarity, suggesting insulin precipitation at the injection site (Fig. 3A). The pH within the injection compartment approached neutrality by ~75 min, correlating with the release of insulin into the infinite sink. These data suggest that insulin formulated in this way rapidly precipitates at the SC injection site and that *m*-cresol can leave the injection site prior to the recovery of insulin solubility and release into the infinite sink. From this data, one could conjecture that some proteins, such as insulin in a crystalline form, could be retained at the SC injection site until conditions favor protein solubility, but that this time return to soluble conditions may occur in the absence of stabilizing excipient(s) present in the drug product.

We next questioned the potential role of ECM elements to affect the release of insulin from the injection chamber. Insuman Comb 50, an insulin suspension formulation designed to provide rapid and intermediate pharmacological actions on blood sugar regulation, was injected into chambers with or without 5 mg/mL HA (Fig. 3B). The release profile of insulin was slowed by the presence of HA in the injection chamber, but the extent of insulin release reached a similar diffused fraction asymptote both with and without the presence of HA. These results suggested that the increased viscosity due to the presence of a HA may slow the release of insulin from the injection chamber but that the extent of insulin release is ultimately not limited by potential interactions with this ECM element. The incomplete diffused fraction (~60%) of the insulin in both cases is most likely due to the slow and incomplete dissolution of the crystalline insulin

in the Insuman Comb 50 formulation. Further, we observed a greater variability in the diffused fractions obtained for the Insuman Comb 50 formulation when it was injected into cassettes lacking HA than into those containing 5% HA. We believe this was because the presence of ECM components the cassette provides a resistance of spreading for the injected formulation, resulting in more consistent outcomes.

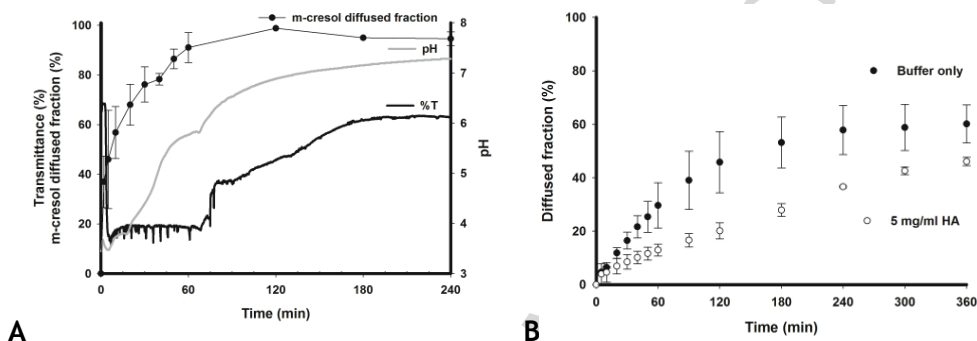


Figure 3. Insulin formulation outcomes in the Scissor system. A) A composite graph showing real-time dynamic changes in pH and percent light transmission (%T) as an index of protein solubility in the injection chamber as well as total amount of an excipient observed in the infinite sink for a test insulin formulation over time. Note how the tracings demonstrate injection chamber acidification and protein precipitation upon its introduction. Protein solubility recovered as the pH in the injection chamber approached neutrality, but at a time when the excipient m-cresol had already left the injection chamber. B) Release rates of insulin from the injection chamber following introduction of Insuman 50 in the presence or absence of 5 mg/mL HA. The data represents average ($n=3$) \pm S.D.

Evaluation of human monoclonal antibody (mAb) formulations using the Scissor system

Four human mAbs having distinct physicochemical properties and formulations (Table 1) were examined. Importantly, previous clinical use of these antibodies has generated bioavailability information following SC injection (in-house data generated by

Genentech): mAb A (77%) > mAb 2 (50-70%) > mAb F (44%) ~ mAb T (42%). The diffused fraction for all of these mAbs from the injection chamber in the absence of HA was 100% (Fig. 4). We examined the release of these mAbs from the injection chamber into the infinite sink compartment as a correlative to release from the SC injection site. Potential interactions of these mAbs with HA was evaluated by examining their movement from the injection chamber to the infinite sink compartment (release profiles) with different levels of HA present in the injection chamber. To enable meaningful comparisons, the highest recovery obtained for each mAb formulation was considered as 100%, with lower recoveries normalized to this value (Fig 4).

Table 1. Properties of the monoclonal antibody (mAb) proteins and formulations used in these studies.

mAb Name	^a Isoelectric Point (pI)	^b Charge at pH 7.4	Concentration in mg/mL	Formulation and pH	^c Formulation Viscosity
mAb A	6.1	-5.3	125	30 mM Histidine-based buffer, pH 5.7	7
mAb 2	7.6	+1.0	125	30 mM Histidine-based buffer, pH 6.0	80
mAb F	8.7	+9.0	150	200 mM Arginine-based buffer, pH 5.5	12
mAb T	9.1	+13	150	200 mM Arginine-based buffer, pH 5.5	5

^aMeasured by isoelectric focusing. ^bTheoretical calculation. ^cDetermined using a cone and plate rheometer and presented as centipoise.

The diffusion profiles for each mAb were affected to varying extents by increased HA concentrations in the injection chamber. This is shown in Figs. 4A-D where the time-concentration diffusion profiles fitted to sampling data points based on Equation 1 for the different mAbs are presented. The diffused fraction of A (Fig. 4A) was not correlated with HA concentration: 5 mg/ml HA content resulted in a lower diffused

fraction than 10 mg/ml HA content (~60 and 80%, respectively). These results suggest that factors other than HA interactions may dominate events that control the release of this antibody from the SC injection site. Data collected for mAb 2 (Fig. 4B) showed a decrease in diffused fraction that correlated with increased HA concentration: 0 (~100% diffused) to 1mg/ml (~90%) to 5 mg/ml (80% diffused), and 10 mg/mL HA resulting to a diffused fraction of ~60% by 6 h.

The addition of HA at 1 mg/ml into the cassette did not hinder the diffusion of mAb F (Fig. 4C). However, addition of HA at 5 and 10 mg/ml concentrations resulted in the diffused fraction decreasing to ~60%. Studies with mAb T (Fig. 4D) showed a gradual decrease in diffused fraction over the HA concentrations tested; its value of ~40% diffused fraction at 6 h at 10 mg/ml HA was similar to that observed for mAb F. It should be noted that triplicate runs yielded highly reproducible results for all HA concentration conditions tested for mAb T and mAb F, suggesting that the basis for antibody interaction with this ECM element was consistently replicated for each test performed (Figs. 4C, 4D). As mAb T and mAb F are positively charged at pH 7.4 (Table 1), the consistency of the data from run-to-run indicate that the retention of these mAbs at the injection site in the presence of HA, which is negatively charged at a physiological pH, could involve electrostatic interactions.

Diffused fraction data obtained for mAb2 without HA or where HA was present at 1 mg/mL were very reproducible but injection of mAb2 into 5 mg/mL HA showed greater variability (Fig. 4B). Further, mAb 2 tested in 10 mg/mL HA was even more variable than the data set obtained for 5 mg/mL HA and was repeated four times. As this antibody is nearly neutral in charge at pH 7.4 (Table 1), the variability could be due to the weakness of electrostatic interactions between the protein and the HA; small changes in the pH for example may result in a significant alteration of the mAb surface charge. Interestingly, these results also correlate with findings from an *in vivo* study in mini-pigs, where a higher pI of an mAb, i.e. higher positive charge at physiological pH,

resulted to lower bioavailability⁵. Furthermore, while mAb A showed reproducible diffused fraction outcomes when tested without HA, the variability in diffusion fraction for this antibody was remarkable for all concentrations of HA tested, requiring five replicates to be performed (Fig. 4A). In contrast to the other antibodies examined in these studies, mAb A failed to show an HA concentration-dependent interaction profile, even though the overall extent of release from the injection chamber was diminished by the presence of HA. Interestingly, this mAb has a net negative charge at neutral pH, and therefore the high variability of our results could reflect electrostatic repulsion between HA and the mAb A molecules whereby release of the antibody from the cassette is dictated by distribution following injection to a greater extent than when antibody-matrix interactions occur through electrostatic attraction.

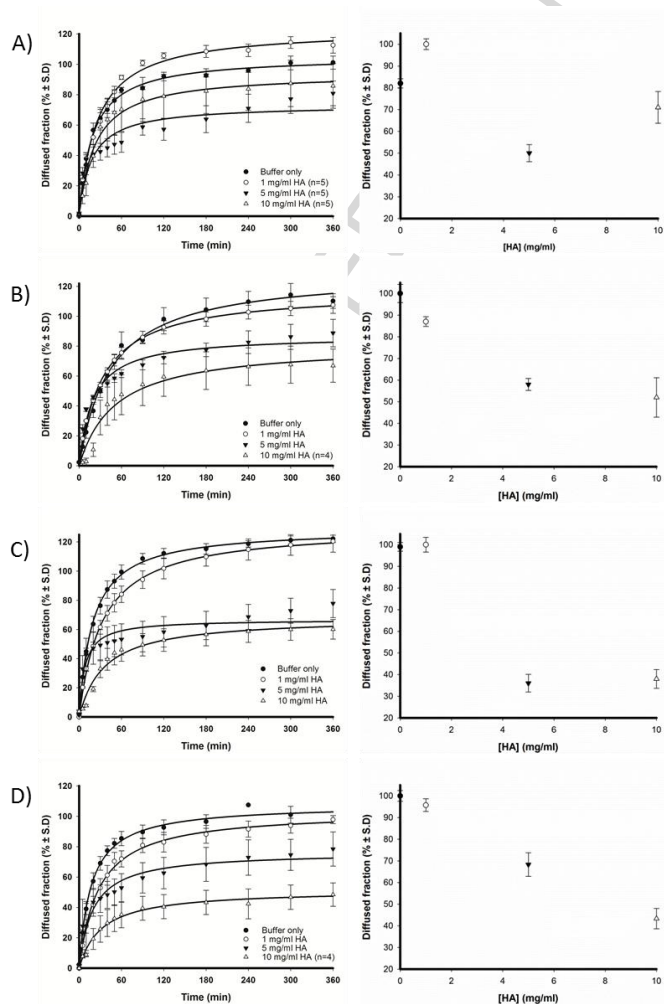


Figure 4. Diffusion of various mAbs from the Scissor system injection chamber containing different concentrations of hyaluronic acid (HA). All mAbs were introduced into the injection chamber as 500 μ L of a formulation with a protein concentration from 125 - 150 mg/mL. The extent of mAb released (A-D; mAbs A, 2, F, and T, respectively) from the injection chamber was determined by SE-HPLC analysis of samples collected from the infinite sink chamber at specific times. Data obtained when the injection chamber contained physiological buffer only (filled circles), or physiological buffer containing 1 mg/mL (open circles), 5 mg/mL (filled triangles), or 10 mg/mL (open triangles) HA are shown as mean values \pm SD. N=3 except where noted otherwise in the legend.

To further study the significance of HA interactions on the extent of mAb release, HAase was injected into the injection chamber 120 min after the introduction of mAb T. Subsequent increase in the diffused fraction of mAb T was observed (Fig. 5A). This finding, in conjunction with data showing increased HA diffusion from the injection site following HAase addition (Fig. 2B), confirms that non-specific interactions between mAb T and HA indeed influence the extent of its release.

Introduction of a long-acting insulin formulation resulted in a rapid lowering of the injection chamber pH and the formation of a precipitate that lowered the %T of the system; transient events where the recovery of physiological pH correlated with an increase in %T and insulin release from the injection chamber (Fig. 3). We questioned whether the moderately acidic formulations of the mAbs tested herein would also demonstrate a decrease in %T and pH transition that might correlate with decreased fraction release outcomes. All of the mAb formulations tested exhibited only a moderate drop in the injection chamber pH with a fairly rapid recovery and none of these formulations demonstrated a reduction in %T in the injection chamber. An example outcome of these studies is shown for mAb T under the conditions of 5 mg/mL HA in the injection chamber that resulted in a transient depression in pH (from 7.4 to ~6.8) and no appreciable decrease in %T (Fig. 5B).

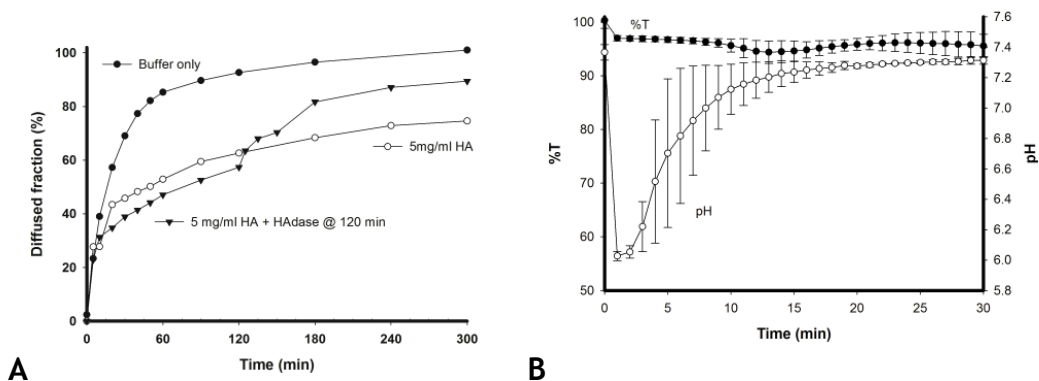


Figure 5. Effect of hyaluronidase (HADase) on mAb release from an injection cassette. A)

Addition of HADase at 2 h into the cassette containing 5 mg/mL HA increased the released fraction of mAb T (inverted triangles) compared to reference experiments at 5 mg/mL HA where no HADase was added (open circles). For comparison, to illustrate the significance of presence of HA into the diffused fraction of mAb T, the release profile for buffer only experiment is also shown (black dots). The data represents mean from 3 experiments. For clarity of presentation error bars have been omitted. B) %T and pH for mAb T formulation with 5 mg/mL HA in the cassette. Data points \pm S.D, n=3.

We next explored parameters that could be used to correlate the properties of mAb release from the injection chamber with the %BA measured for these proteins in patients. In plotting the fraction of dose released at the 6 h plateau for the different HA concentrations tested, a pattern of HA dependence for these four mAbs emerged that showed a correlation between *in vivo* %BA and the diffused fraction of the mAbs, where 10 mg/mL HA was included in the injection chamber (Fig. 6A). Variability of Scissor system outcomes must be comparable to the variability of *in vivo* %BA outcomes for such a correlate to be meaningful. We performed a t-test and an f-test analysis; there was no statistically significant difference between the distributions or variability of these data (note that variability data for mAb 2 in patients was not available and thus not included). A linear regression analysis showed a goodness of fit ($R^2 = 0.93$ and a slope of -1 that demonstrated a good correlation between 10% HA outcome and %BA outcomes in

patients for these four mAb (Fig. 6B). Thus, our data supports the potential role of HA interactions as an ECM element that could affect the absorption of these four human mAbs from a SC injection site.

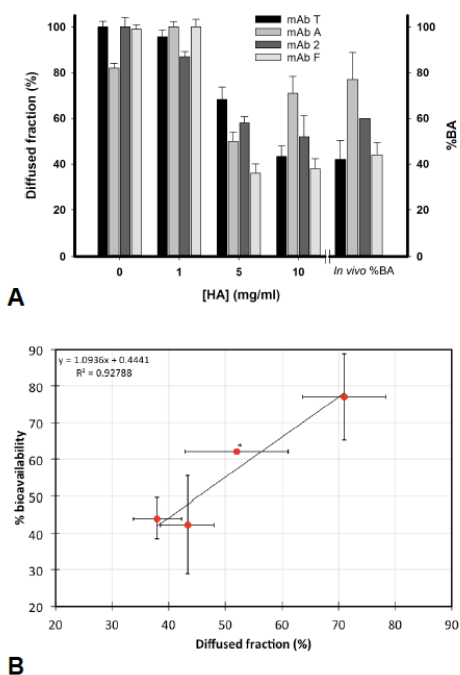


Figure 6. Correlation of injection chamber HA concentration with diffused fraction release and human bioavailability. A) Fraction release of mAbs from the injection chamber at 6 h as a function of HA concentration (mg/mL) and comparison to %BA values observed in humans. B) Linear regression analysis between Scissor values and human %BA outcomes presented in A).

CONCLUSIONS AND PERSPECTIVES

Despite extensive clinical use, the exact mechanism underlying subcutaneous absorption of protein and peptide drugs is still poorly understood, with their absorption in patients being relatively slow and mostly incomplete^{26,27}. Presently, there is no animal model that can reliably predict clinical pharmacokinetics²⁸. We have begun to address this deficiency by developing an *in vitro* system (Scissor) that uses a dialysis membrane-restricted compartment that contains selected and defined ECM elements present in the

hypodermis, to model potential events and interactions that might occur following SC injection of a biopharmaceutical formulation. This system establishes physiologically relevant conditions for temperature and pressure, while allowing for the dynamic transition of environmental conditions of a biopharmaceutical from its drug product formulation to conditions perceived to be present in the hypodermis¹⁶.

Many of the previous studies examining biopharmaceutical uptake following SC injection have focused on defining the relative contributions of lymph versus blood uptake from hypodermis^{26,27}. The Scissor system is focused on events within the hypodermis and not the route by which materials might leave the SC injection site. The dialysis membrane used in the Scissor system was prepared in a way to emulate the mixture of diffusion and blood/lymph capillary uptake that define the major mechanisms involved in movement of a biopharmaceutical from a SC injection site and thus does not attempt to discriminate between the two; this membrane was shown to provide linearity relative to molecular weight. The injection chamber can be prepared with different mixtures of acellular ECM components that are retained by this dialysis membrane for the duration of these studies and used to assess the impact of these materials on a SC injection formulation in a tractable manner.

Our initial studies have demonstrated how excipients can leave the injection chamber before the biopharmaceutical, how a biopharmaceutical can initially precipitate after injection and then release from the injection site after equilibration following pH recovery that leads to resolubilization, and how an ECM element can slow or modify the release of a biopharmaceutical at the injection site. Studies involving insulin and a series of monoclonal antibodies were described in this report, but other peptides and protein therapeutics as well as small molecule drug formulations designed for sustained release could be assessed using the Scissor system. With regard to the latter, we are now fitting the Scissor system with a digital camera to allow visual characterization of formulation performance.

The Scissor system allows monitoring the rate and status of individual components of a formulation to examine their fate after introduction into an acellular hypodermis-like environment that returns to the homeostatic conditions of the hypodermis. Importantly, clinically-relevant of formulation volumes and drug doses can be introduced into the injection chamber for testing. Sampling of the infinite sink compartment allows information to be gathered regarding the extent and condition of materials leaving the injection chamber. Monitoring events within the injection chamber can be performed using visible light spectroscopy as we have identified, as HA is optically clear. Although removal of injection chamber material at specific times to assess events occurring at this artificial injection site can provide valuable information, we have focused on methods of non-invasive assessment of the injection chamber. The current version of the Scissor system is capable of providing real time information of events within the injection chamber and we aim to develop other integrated tools to provide additional real time data, such as Raman spectroscopy.

The Scissor system is not intended to reproduce the entirety or complexity of events that occur at the SC injection site or to directly replicate individual components of the hypodermis. Further, the exact composition of ECM elements in the hypodermis is unclear. HA concentration in the human dermis has been determined to be 0.2 mg/g²⁹, which is probably less than that present in the hypodermis; it is unclear, however, if HA levels in the hypodermis reach 10 mg/mL, as used in our studies. Importantly, Scissor is designed to provide a tractable system where specific interactions can be explored and these studies have supported the use of an *in vitro* format using up to 10 mg/mL of HA to discern potential interactions for this ECM component. The system is not sterile and can realistically be run under physiological conditions for only up to about 12 h. Longer studies can be performed with the addition of a bacterial static agent, but this addition compromises the physiological basis of the method and the outcomes must be

considered accordingly. The acellular nature of the current Scissor system limits the acquisition of information regarding local cell-based metabolic events that might at the injection site for highly potent biopharmaceuticals that are administered at low doses³⁰.

One of the first steps in the development of a biopharmaceutical involves the identification of a formulation that ensures a multi-year shelf-life required for commercial success. Often, several types of formulations can provide the desired shelf-life stability and the ultimate selection between these must be made based upon *in vivo* animal studies that may or may not reflect subsequent outcomes in man³¹. There is no method to compare multiple formulations that will predict pharmacokinetics and other clinical outcomes and clinical testing of multiple formulations is prohibitively expensive. The Scissor system can provide a useful *in vitro* rapid screening tool to assess potential injection site outcomes, as an early step in formulation development and selection that would reduce animal use, expedite the formulation selection process, and provide a tractable method for the optimization of formulations. Overall, our data suggest the Scissor system to provide a robust, rapid, and tractable *in vitro* system to model potential events following SC injection. Ultimate benefit of the Scissor system to medicine could come in several forms: expedited testing of candidate formulations without using animals to rapidly and efficiently identify those most appropriate for further pre-clinical screening, rational improvements in therapeutics and formulations designed for SC injection identified through a reproducible and systematic screening effort, and the possibility of defining parameters to assess consistency of performance for a marketed formulation administered by SC injection. We believe such a tool could also lead to hypothesis-driven testing to better define specific aspects of hypodermis biology.

Acknowledgements

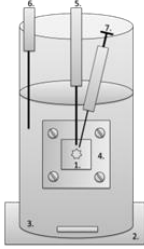
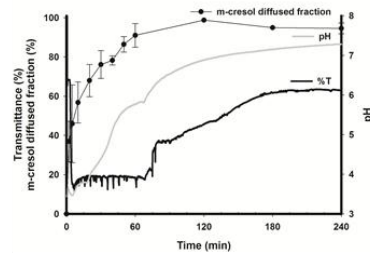
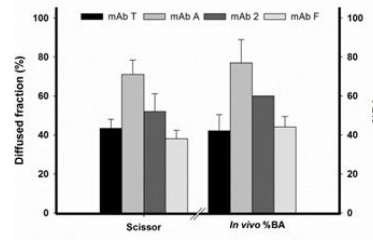
RJM thanks the Wellcome Trust for being a VIP recipient. This work was partially supported by funding from the SARTE Bio-e initiative, and the University of Bath. Yafei Yu and Yu Bingcheng were funded by the Bath-Shangdong Pharmacy and Pharmacology Scholarship Program. Sirius Analytical Instruments Ltd are acknowledged for an ongoing collaboration.

REFERENCES

1. Escudier, B. Metastatic RCC: moving towards a chronic disease. *Oncology* **26**, 304, 306 (2012).
2. Pivot, X., *et al.* Preference for subcutaneous or intravenous administration of trastuzumab in patients with HER2-positive early breast cancer (PrefHer): an open-label randomised study. *The Lancet. Oncology* **14**, 962-970 (2013).
3. Tang, L., Persky, A.M., Hochhaus, G. & Meibohm, B. Pharmacokinetic aspects of biotechnology products. *Journal of pharmaceutical sciences* **93**, 2184-2204 (2004).
4. Wang, W., Wang, E.Q. & Balthasar, J.P. Monoclonal antibody pharmacokinetics and pharmacodynamics. *Clinical pharmacology and therapeutics* **84**, 548-558 (2008).
5. Mach, H. & Arvinte, T. Addressing new analytical challenges in protein formulation development. *European journal of pharmaceuticals and biopharmaceutics : official journal of Arbeitsgemeinschaft fur Pharmazeutische Verfahrenstechnik e.V* **78**, 196-207 (2011).
6. Bleuel, H., *et al.* Kinetics of subcutaneous versus intravenous epoetin-beta in dogs, rats and mice. *Pharmacology* **52**, 329-338 (1996).
7. Macdougall, I.C., Roberts, D.E., Coles, G.A. & Williams, J.D. Clinical pharmacokinetics of epoetin (recombinant human erythropoietin). *Clinical pharmacokinetics* **20**, 99-113 (1991).
8. Salmonson, T., Danielson, B.G. & Wikstrom, B. The pharmacokinetics of recombinant human erythropoietin after intravenous and subcutaneous administration to healthy subjects. *British journal of clinical pharmacology* **29**, 709-713 (1990).
9. Gibson, D.M., Cotler, S., Spiegel, H.E. & Colburn, W.A. Pharmacokinetics of recombinant leukocyte A interferon following various routes and modes of administration to the dog. *Journal of interferon research* **5**, 403-408 (1985).
10. Wills, R.J. Clinical pharmacokinetics of interferons. *Clinical pharmacokinetics* **19**, 390-399 (1990).
11. Oussoren, C. & Storm, G. Liposomes to target the lymphatics by subcutaneous administration. *Advanced drug delivery reviews* **50**, 143-156 (2001).
12. Porter, C.J., Edwards, G.A. & Charman, S.A. Lymphatic transport of proteins after s.c. injection: implications of animal model selection. *Advanced drug delivery reviews* **50**, 157-171 (2001).
13. Supersaxo, A., Hein, W.R. & Steffen, H. Effect of molecular weight on the lymphatic absorption of water-soluble compounds following subcutaneous administration. *Pharmaceutical research* **7**, 167-169 (1990).
14. Muchmore, D.B. & Vaughn, D.E. Accelerating and improving the consistency of rapid-acting analog insulin absorption and action for both subcutaneous injection and continuous subcutaneous infusion using recombinant human hyaluronidase. *Journal of diabetes science and technology* **6**, 764-772 (2012).
15. Shpilberg, O. & Jackisch, C. Subcutaneous administration of rituximab (MabThera) and trastuzumab (Herceptin) using hyaluronidase. *British journal of cancer* **109**, 1556-1561 (2013).

16. Kinnunen, H.M. & Mørn, R.J. Improving the outcomes of biopharmaceutical delivery via the subcutaneous route by understanding the chemical, physical and physiological properties of the subcutaneous injection site. *Journal of Controlled Release* **182**, 22-32 (2014).
17. Ogamo, A., Matsuzaki, K., Uchiyama, H. & Nagasawa, K. Preparation and properties of fluorescent glycosaminoglycuronans labeled with 5-aminofluorescein. *Carbohydrate research* **105**, 69-85 (1982).
18. Kay, M.D., *et al.* Static normothermic preservation of renal allografts using a novel nonphosphate buffered preservation solution. *Transplant international : official journal of the European Society for Organ Transplantation* **20**, 88-92 (2007).
19. Agency, E.M. Insulin preparations, injectable: European Medicines Agency. *European Pharmacopoeia*, 1808-1811 (2005).
20. Aukland, K. & Reed, R.K. Interstitial-lymphatic mechanisms in the control of extracellular fluid volume. *Physiological reviews* **73**, 1-78 (1993).
21. Fogh-Andersen, N., Altura, B.M., Altura, B.T. & Siggaard-Andersen, O. Composition of interstitial fluid. *Clinical chemistry* **41**, 1522-1525 (1995).
22. Webb, P. Temperatures of skin, subcutaneous tissue, muscle and core in resting men in cold, comfortable and hot conditions. *European Journal of Applied Physiology and Occupational Physiology* **64**, 471-476 (1992).
23. Noddeland, H. Colloid osmotic pressure of human subcutaneous interstitial fluid sampled by nylon wicks: evaluation of the method. *Scandinavian journal of clinical and laboratory investigation* **42**, 123-130 (1982).
24. Noddeland, H. Influence of body posture on transcapillary pressures in human subcutaneous tissue. *Scandinavian journal of clinical and laboratory investigation* **42**, 131-138 (1982).
25. Birnbaum, D.T., Dodd, S.W., Saxberg, B.E., Varshavsky, A.D. & Beals, J.M. Hierarchical modeling of phenolic ligand binding to 2Zn--insulin hexamers. *Biochemistry* **35**, 5366-5378 (1996).
26. Kagan, L. & Mager, D.E. Mechanisms of subcutaneous absorption of rituximab in rats. *Drug metabolism and disposition: the biological fate of chemicals* **41**, 248-255 (2013).
27. Richter, W.F. & Jacobsen, B. Subcutaneous absorption of biotherapeutics: knowns and unknowns. *Drug metabolism and disposition: the biological fate of chemicals* **42**, 1881-1889 (2014).
28. Zheng, Y., *et al.* Minipig as a potential translatable model for monoclonal antibody pharmacokinetics after intravenous and subcutaneous administration. *mAbs* **4**, 243-255 (2012).
29. Fraser, J.R., Laurent, T.C. & Laurent, U.B. Hyaluronan: its nature, distribution, functions and turnover. *Journal of internal medicine* **242**, 27-33 (1997).
30. Wang, W., *et al.* Lymphatic transport and catabolism of therapeutic proteins after subcutaneous administration to rats and dogs. *Drug metabolism and disposition: the biological fate of chemicals* **40**, 952-962 (2012).
31. Wang, W., *et al.* Immunogenicity of protein aggregates--concerns and realities. *International journal of pharmaceutics* **431**, 1-11 (2012).

Subcutaneous injection site simulator (Scissor)

*In situ* data*In vitro – in vivo* relationship

Graphical abstract